Adaptive perfectly matched layer method for multiple scattering problems[☆]

Xue Jiang[a], Weiying Zheng[a,*]

[a]LSEC, Institute of Computational Mathematics, Academy of Mathematics and Systems Science, Chinese Academy of Sciences, Beijing 100190, China.

Abstract

A uniaxial perfectly matched layer (UPML) method is proposed for solving three-dimensional Helmholtz equation with multiple scatterers. The exterior domain is truncated to enclose each scatterer by a bounded domain individually. Based on reliable a posteriori error estimate, an efficient adaptive finite element algorithm is proposed to solve the multiple scattering problem. The efficiency of the adaptive PML method is demonstrated by extensive numerical experiments.

Keywords: Uniaxial perfectly matched layer, multiple scattering problems, adaptive finite element, a posteriori error estimate.
2000 MSC: 65N30, 35J05

1. Introduction

We propose and study an adaptive uniaxial perfectly matched layer method for multiple scattering problems in three dimensions

$$\Delta u + k^2 u = 0 \qquad \text{in} \quad \mathbb{R}^3 \setminus \overline{D}, \tag{1a}$$

$$u = g \qquad \text{on} \quad \partial D, \tag{1b}$$

$$\lim_{r=|\boldsymbol{x}|\to\infty} r\left|\frac{\partial u}{\partial r} - \mathbf{i}k\, u\right| = 0, \tag{1c}$$

where k is the constant wave number and $g \in H^{1/2}(\partial D)$. The scatterer $D \subset \mathbb{R}^3$ consists of well-separated sub-scatterers which are bounded and have Lipschitz boundaries (see Fig. 1 for a 2D illustration), namely, $D = \cup_{i=1}^{I} D_i$ and

$$\mathrm{dist}(D_i, D_j) := \sup_{\boldsymbol{x}\in D_i, \boldsymbol{y}\in D_j} |\boldsymbol{x} - \boldsymbol{y}| \gg \mathrm{diam}(D_i) + \mathrm{diam}(D_j) \qquad \forall\, 1 \le i < j \le I.$$

[☆]This work was supported in part by China NSF (Grant No. 60873177, 11031006) and the Funds for Creative Research Groups of China (Grant No. 11021101).

[*]Corresponding author: +86-10-62625224 (Tel), +86-10-62542285 (Fax).

Email addresses: jxue@lsec.cc.ac.cn (Xue Jiang), zwy@lsec.cc.ac.cn (Weiying Zheng)

For the numerical solution of (1), it is usual to truncate the exterior of D to a bounded domain which encloses all sub-scatterers and inhomogeneities of the medium. There are extensive works studying approximate boundary conditions of scattering problems on the artificial boundary (cf. e.g. [1, 2, 3]). However, when $D_1, \cdots, D_I$, $I > 1$ are well-separated, the truncated domain is so large that the numerical solution of (1) becomes very expensive. In [4], Grote and Kirsch proposed to enclose the sub-scatterers by separate domains $B_i \supset \overline{D}_i$ such that $B_i \cap B_j = \emptyset$ for $i \neq j$. They constructed a Dirichlet-to-Neumann (DtN) boundary condition on each ∂B_i and solved a boundary value problem in $\cup_{i=1}^{I} \left(B_i \setminus \overline{D}_i\right)$. One can expect much less unknowns from the discretization of the problem in $\cup_{i=1}^{I} \left(B_i \setminus \overline{D}_i\right)$ than that in the globally truncated domain.

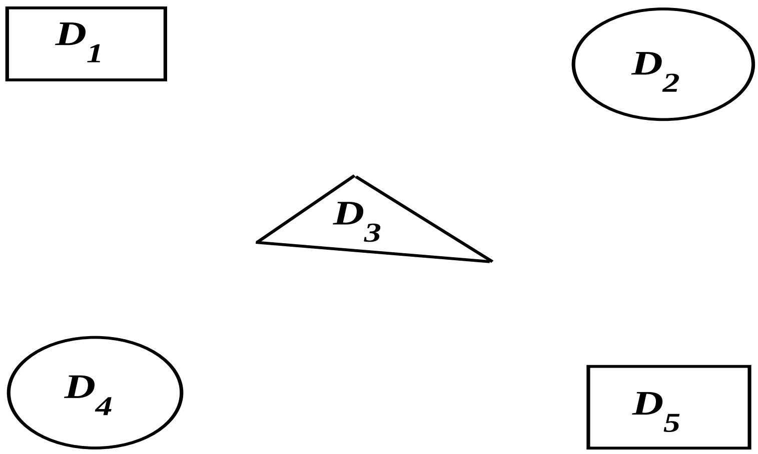

Figure 1: A 2D illustration for the setting of the multiple scattering problem.

In this paper, we propose to study the adaptive UPML finite element method for solving the multiple scattering problem (1). Since the pioneering work of Bérenger [5] which proposed a UPML method for solving the time dependent Maxwell equations, various constructions of PML absorbing layers have been developed and studied in the literature (cf. e.g. Turkel and Yefet [6], Teixeira and Chew [7] for the reviews). The basic idea of the PML method is to surround the computational domain by a layer of specially designed model medium which absorbs all waves coming from the computational domain. The PML method provides a highly accurate boundary condition on the truncated boundary and avoids dense blocks of the stiffness matrix which are caused by the discrete DtN operator. The convergence of the PML method as the thickness of the layer tends to infinity has drawn considerable attentions in the literature (cf. e.g. [8, 9]).

In the practical application of PML methods, Chen and coauthors proposed the adaptive PML (APML) method for acoustic and electromagnetic scattering problems (see [10, 11, 12]). The APML method provides a complete numerical strategy to solve the scattering problems in the framework of finite elements. It produces automatically a coarse mesh size away from the fixed domain and thus makes the total computational costs insensitive to the thickness of the PML absorbing layer. The main idea of the APML method is to use the a posteriori error estimate to determine the PML parameters and to use the adaptive finite element method to solve the PML equations.

In [13], Guddati and Lim proposed a continued fraction absorbing boundary condition (CFABC) for convex polygonal domains. The CFABC method and the PML method provide respectively a discrete approximation and a continuous approximation to the original scattering problem. They only produce very small reflections at the truncated boundary of the infinity space. The PML method is very flexible in designing numerical schemes (e.g. on adaptively refined meshes or for high-order approximations), but may produce numerical reflections because of discretization errors. Numerical reflections can be reduced efficiently by improving the accuracy of numerical methods for the PML problem. We refer to [14, 15] for the improvement of PML methods by hp-adaptive finite element methods. In this paper, we only focus on h-adaptive PML methods for multiple scattering problems.

For multiple scattering problems, one could not simply impose homogeneous Dirichlet boundary condition on the truncated boundary of the PML surrounding each B_i, since there are both outgoing waves coming from D_i and incoming waves scattered by other sub-scatterers across ∂B_i, $1 \leq i \leq I$. In fact, the PML medium surrounding B_i absorbs the waves from D_i but enhances the waves from other sub-scatterers. We decompose the total scattering field into the addition of the scattering waves from each individual sub-scatterer. Then surrounding each sub-scatterer, we construct a layer of wave-absorbing medium to damp the outgoing waves from it. We proved that the solution of the PML problem converge exponentially to the exact solution of (1) as either the thickness of the layers or the medium properties increase. For the conforming finite element approximation of the PML problem, we propose an APML algorithm based on reliable a posteriori error estimates.

The stiffness matrix of the system of algebraic equations has dense blocks produced by the wave propagation operators. This makes the system hard to solve. We propose a block Gauss-Seidel method for the solution of the system of algebraic equations. The block Gauss-Seidel method is equivalent to an alternative iteration method for the discrete problem. Based on this observation, we propose an alternative APML (AAPML) method. In the procedure of adaptive iterations, the stiffness matrices of the AAPML method are sparse and independent of the DtN operators and the wave propagation operators. In the last section, we present some numerical experiments to demonstrate the efficiency of the AAPML method.

The layout of the paper is as follows. In Section 2, we prove that the solution of (1) can be uniquely decomposed into the addition of purely outgoing waves from each individual sub-scatterers. In Section 3, we study the PML finite element method for single scattering problems. In Section 3.2, we introduce the conforming finite element approximation to the PML problem. Reliable a posteriori error estimate is derived to control both the thickness of the PML and the mesh refinements. In Section 4, we adopt the theories for single scattering problems to multiple scattering problems to prove the exponential convergence of the PML method and to derive the a posteriori error estimate. In Section 5, we proposed an alternative iteration method for the solution of the coupled system. In Section 6, we proposed the APML and AAPML algorithms for the multiple scattering problem. Three numerical experiments are also presented to demonstrated the efficiency of the AAPML algorithm.

2. Regular decomposition of the multiple scattering field

Let u be the solution of (1) and $G(\boldsymbol{x},\boldsymbol{y}) = \frac{e^{\mathbf{i}k|\boldsymbol{x}-\boldsymbol{y}|}}{4\pi|\boldsymbol{x}-\boldsymbol{y}|}$ be the fundamental solution satisfying

$$\Delta G(\boldsymbol{x},\boldsymbol{y}) + k^2 G(\boldsymbol{x},\boldsymbol{y}) = -\delta(\boldsymbol{x},\boldsymbol{y}). \tag{2}$$

By the Kirchhoff-Helmholtz formula (see e.g. [17, Theorem 2.4]), u has the following representation:

$$u(\boldsymbol{x}) = \int_{\partial D}\Big(\frac{\partial G(\boldsymbol{x},\boldsymbol{y})}{\partial \boldsymbol{n}_{\boldsymbol{y}}}u(\boldsymbol{y}) - \frac{\partial u(\boldsymbol{y})}{\partial \boldsymbol{n}}G(\boldsymbol{x},\boldsymbol{y})\Big)\mathrm{d}s_{\boldsymbol{y}} = \sum_{i=1}^{I} u_i(\boldsymbol{x}) \quad \forall\, \boldsymbol{x}\in\mathbb{R}^3\setminus\overline{D}, \tag{3}$$

where $\boldsymbol{n}$ is the unit outer normal of ∂D and

$$u_i(\boldsymbol{x}) = \int_{\Gamma_i}\Big(\frac{\partial G(\boldsymbol{x},\boldsymbol{y})}{\partial \boldsymbol{n}_{\boldsymbol{y}}}u(\boldsymbol{y}) - \frac{\partial u(\boldsymbol{y})}{\partial \boldsymbol{n}}G(\boldsymbol{x},\boldsymbol{y})\Big)\mathrm{d}s_{\boldsymbol{y}}, \qquad \Gamma_i = \partial D_i. \tag{4}$$

From (2) and (4) we deduce that u_i solves the following scattering problem:

$$\begin{cases} \Delta u_i + k^2 u_i = 0 & \text{in } \mathbb{R}^3\setminus\overline{D_i}, \\ u_i = g - \sum_{j=1,j\neq i}^{I} u_j & \text{on } \Gamma_i, \\ \lim_{r\to\infty} r\left|\frac{\partial u_i}{\partial r} - \mathbf{i}k\, u_i\right| = 0, \end{cases} \qquad \forall\, 1\le i\le I. \tag{5}$$

Clearly (5) is a system of I scattering problems which are coupled by the Dirichlet boundary conditions.

Theorem 2.1. *Let u be the unique solution to problem (1) and u_i, $1\le i\le I$ solve* (5). *Then $u = \sum_{i=1}^{I} u_i$ is the unique decomposition of u into purely outgoing waves.*

Proof. The idea is drawn from the proof of [4, Proposition 1]. From (3), we need only prove the uniqueness of the decomposition. By induction, it is sufficient to consider the case of $I = 2$. We let $u = v_1 + v_2$ be another decomposition in $\mathbb{R}^3\backslash\overline{D}$ where v_1, v_2 solve (5). Then $w_i = u_i - v_i$ satisfies

$$\Delta w_i + k^2 w_i = 0 \ \text{ in } \ \mathbb{R}^3\setminus\overline{D_i} \quad \text{and} \quad \lim_{r\to\infty} r\left|\frac{\partial w_i}{\partial r} - \mathbf{i}k\, w_i\right| = 0, \qquad i = 1,2.$$

Since D_1, D_2 are well-separated, without loss of generality, we can assume that $\overline{D}_1 \subset B(0,R) \subset B(0,2R) \subset \mathbb{R}^3\setminus\overline{D}_2$ where $B(0,R)$ is the ball of radius R and centering at the origin.

By the interior regularity of elliptic problems, w_i, $i = 1,2$, are regular in $\mathbb{R}^3\setminus\overline{D}_i$ and admit the following expansion in the vicinity of $\partial B(0,R)$

$$\begin{aligned} w_1(r,\theta,\phi) &= \sum_{l=0}^{\infty}\sum_{m=-l}^{l} a_{lm} H_l^{(1)}(kr) Y_l^m(\theta,\phi), \\ w_2(r,\theta,\phi) &= \sum_{l=0}^{\infty}\sum_{m=-l}^{l} b_{lm} J_l(kr) Y_l^m(\theta,\phi). \end{aligned}$$

The uniqueness of u implies that $w_1 + w_2 = 0$ in $\mathbb{R}^3 \backslash \overline{D}$. Thus

$$a_{lm} H_l^{(1)}(kr) + b_{lm} J_l(kr) = 0, \qquad \forall\, l \geq 0, \;\; -l \leq m \leq l, \;\; R \leq r \leq 2R. \tag{6}$$

Since $H_l^{(1)}$ and J_l are linearly independent, we have $a_{lm} = b_{lm} = 0$ for all $l \geq 0$ and $-l \leq m \leq l$. Thus $w_1 = w_2 = 0$ in $B(0, 2R) \setminus \overline{B(0, R)}$. By the unique continuity principle (see [17, Lemma 8.5] and [18, Lemma 4.15]), we conclude $v_1 \equiv u_1$ and $v_2 \equiv u_2$ in $\mathbb{R}^3 \backslash D$. □

3. PML finite element method for single scattering problems

Notice that (5) is a system of single scattering problems. This purpose of this section is to study the PML finite element method for single scattering problems which plays a key role in the PML finite element method for (1). Since most of the proofs in this section run parallel with the two-dimensional case, we only present the main results and refer to [12] for the detailed proofs.

For convenience we omit the superscripts and subscripts and write (5) into the general single-scattering problem:

$$\begin{cases} \Delta w + k^2 w = 0 & \text{in} \;\; \mathbb{R}^3 \setminus \overline{S}, \\ w = f_S & \text{on} \;\; \partial S, \\ \lim_{r\to\infty} r \left| \frac{\partial w}{\partial r} - \mathbf{i} k\, w \right| = 0, \end{cases} \tag{7}$$

where $w = u_i$, S stands for the sub-scatterers D_i, $1 \leq i \leq I$, and f_S stands for any of the Dirichlet boundary conditions in (5). Without loss of generality, we assume that S nears the origin and introduce a truncated domain $B := (-L_1, L_1) \times (-L_2, L_2) \times (-L_3, L_3)$ such that $\overline{S} \subset B$. By the Kirchhoff-Helmholtz formula (see e.g. [17, Theorem 2.4]), w has the following representation:

$$w(\boldsymbol{x}) = \int_{\partial B} \Big(\frac{\partial G(\boldsymbol{x}, \boldsymbol{y})}{\partial \boldsymbol{n}_{\boldsymbol{y}}} w(\boldsymbol{y}) - \frac{\partial w(\boldsymbol{y})}{\partial \boldsymbol{n}} G(\boldsymbol{x}, \boldsymbol{y}) \Big) \mathrm{d}s_{\boldsymbol{y}} \qquad \forall\, \boldsymbol{x} \in \mathbb{R}^3 \setminus \overline{B}. \tag{8}$$

3.1. The PML problem

To introduce the absorbing PML for problem (7), we define a larger box

$$O = \{\boldsymbol{x} \in \mathbb{R}^3 : |x_m| < L_m + d_m, \;\; 1 \leq m \leq 3\}.$$

Let $\alpha_m(t) = 1 + \mathbf{i}\sigma_m(t)$ be the model medium property of the PML surrounding B, where

$$\sigma_m(t) = \begin{cases} 0 & \text{if} \;\; |t| \leq L_m, \\ \widetilde{\sigma}_m \left(\frac{|t| - L_m}{d_m} \right)^n & \text{if} \;\; |t| > L_m. \end{cases}$$

Here $\widetilde{\sigma}_m > 0$ is a constant and $n \geq 0$ is an integer. The uniaxial PML is defined by the complex coordinate stretching

$$\widetilde{x}_m = \int_0^{x_m} \alpha_m(t) \mathrm{d}t = x_m + \mathbf{i} \int_0^{x_m} \sigma_m(t) \mathrm{d}t, \quad m = 1, 2, 3, \qquad \forall\, \boldsymbol{x} \in \overline{O}. \tag{9}$$

Clearly the scattering solution propagates as follows in the PML:

$$w(\widetilde{\boldsymbol{x}}) = \int_{\partial B} \Big(\frac{\partial G(\widetilde{\boldsymbol{x}}, \boldsymbol{y})}{\partial \boldsymbol{n}_y} w(\boldsymbol{y}) - \frac{\partial w(\boldsymbol{y})}{\partial \boldsymbol{n}} G(\widetilde{\boldsymbol{x}}, \boldsymbol{y}) \Big) \mathrm{d}s_y \qquad \forall\, \boldsymbol{x} \in \mathbb{R}^3 \setminus \overline{B}. \tag{10}$$

Define $\widetilde{w}(\boldsymbol{x}) := w(\widetilde{\boldsymbol{x}})$ for any $\boldsymbol{x} \in O \setminus \overline{S}$. It is obvious that $\widetilde{w}$ satisfies

$$\frac{\partial^2 \widetilde{w}}{\partial \widetilde{x}_1^2} + \frac{\partial^2 \widetilde{w}}{\partial \widetilde{x}_2^2} + \frac{\partial^2 \widetilde{w}}{\partial \widetilde{x}_3^2} + k^2 \widetilde{w} = 0 \qquad \text{in } \ \Omega := O \setminus \overline{S},$$

which yields the desired PML equation in real coordinates

$$\nabla \cdot (A \nabla \widetilde{w}) + b k^2 \widetilde{w} = 0 \qquad \text{in } \ \Omega, \tag{11}$$

where $A = \operatorname{diag}\left(\frac{\alpha_2 \alpha_3}{\alpha_1}, \frac{\alpha_1 \alpha_3}{\alpha_2}, \frac{\alpha_1 \alpha_2}{\alpha_3} \right)$ is a diagonal matrix and $b = \alpha_1 \alpha_2 \alpha_3$.

In the rest of this paper, we make the following assumption on the fictitious medium property which is rather mild in practical applications of the uniaxial PML method:

(H1) $$\int_{L_1}^{L_1+d_1} \sigma_1(t) \mathrm{d}t = \int_{L_2}^{L_2+d_2} \sigma_2(t) \mathrm{d}t = \int_{L_3}^{L_3+d_3} \sigma_3(t) \mathrm{d}t = \bar{\sigma}.$$

Theorem 3.1. *Let* (H1) *be satisfied and* $\gamma \bar{\sigma} \geq 1$ *with* $\gamma := \frac{\min(d_1, d_2, d_3)}{\sqrt{(2L_1+d_1)^2 + (2L_2+d_2)^2 + (2L_3+d_3)^2}}$. *There exists a constant* $C > 0$ *independent of* $\bar{\sigma}$ *and* d_1, d_2, d_3 *such that*

$$\left\| \widetilde{w} \right\|_{H^{1/2}(\partial O)} \leq C \alpha_0 (1 + kL)^2 e^{-k\gamma\bar{\sigma}} \left\| w \right\|_{H^{1/2}(\partial B)},$$

where $\alpha_0 = \max\limits_{\boldsymbol{x} \in \partial O} \big(|\alpha_1(x_1)|, |\alpha_2(x_2)|, |\alpha_3(x_3)| \big)$.

Proof. The proof depends on the estimate of the modified Green function $G(\widetilde{x}, y)$ and runs parallel with the two-dimensional case. We refer to [12, Section 3.1] for the proof in two dimension and omit the details. □

Theorem 3.1 states that $\widetilde{w}$ decays exponentially in the PML. We define an approximate problem of (7) by setting homogeneous Dirichlet boundary condition on the outer boundary

$$\begin{cases} \nabla \cdot (A \nabla \hat{w}) + b k^2 \hat{w} = 0 & \text{in } \ \Omega, \\ \hat{w} = f_S & \text{on } \ \partial S, \\ \hat{w} = 0 & \text{on } \ \partial O. \end{cases} \tag{12}$$

A weak formulation of (12) is: Find $\hat{w} \in H^1(B \setminus \overline{S})$ such that $\hat{w} = f_S$ on ∂S and

$$\hat{a}(\hat{w}, v) := \int_{B \setminus \overline{S}} \left(\nabla \hat{w} \cdot \nabla \bar{v} - k^2 \hat{w} \bar{v} \right) \mathrm{d}\boldsymbol{x} - \left\langle \widehat{T} \hat{w}, v \right\rangle_{\partial B} = 0 \quad \forall\, v \in H^1_{\partial S}(B \setminus \overline{S}), \tag{13}$$

where for any Lipschitz domain Y and two-dimensional manifold $\Sigma \subset \overline{Y}$, we define

$$H^1_\Sigma(Y) := \{ v \in H^1(Y) : v = 0 \text{ on } \Sigma \}.$$

The DtN operator $\widehat{T}$: $H^{1/2}(\partial B) \mapsto H^{-1/2}(\partial B)$ is defined by $\widehat{T}f := \frac{\partial\eta}{\partial \boldsymbol{n}}$ for any $f \in H^{1/2}(\partial B)$, where η solves

$$\begin{cases} \nabla\cdot(A\nabla\eta) + bk^2\eta = 0 & \text{in } \Omega_{\rm PML}, \\ \eta = f & \text{on } \partial B, \\ \eta = 0 & \text{on } \partial O. \end{cases} \tag{14}$$

Recall that under the complex coordinate stretching, (14) is equivalent to the Helmhotz equation in $\Omega_{\rm PML}$ with Dirichlet boundary conditions. By the spectral theory of compact operators, (14) has a unique solution for all real k except possibly for a countable number of values. The well-posedness of the PML problems has been constructed in [19] for two-dimensional case and in [10, 21] for circular PML methods. But the well-posedness for the UPML problem in three-dimension has retained an interesting open problem. In this paper we will not elaborate on this issue and simply make the following assumption

(**H2**) There exists a unique solution to the Dirichlet PML problem (14) for any $f \in H^{1/2}(\partial B)$.

Theorem 3.2. *Let w be the solution of* (7) *and let* (H1)–(H2) *be satisfied. Then for sufficiently large $\bar\sigma > 0$,the PML problem* (12) *has a unique solution $\hat w \in H^1(\Omega)$. Moreover, there exists a constant C which depends on k and $\bar\sigma$ at most polynomially such that*

$$\|w-\hat w\|_{H^1(B\setminus\overline{S})} \;\leq\; C\alpha_0^3(1+kL)^3e^{-k\gamma\bar\sigma}\,\|\hat w\|_{H^{1/2}(\partial B)}\,. \tag{15}$$

Proof. The proof uses similar arguments as in the proof of [12, Theorem 3.8]. For the sake of simplicity, we do not elaborate on the details here. □

3.2. Finite element approximation to single scattering problems

To study finite element approximations, we introduce another weak formulation of (12): Find $w \in H^1(\Omega)$ such that $w = f_S$ on ∂S, $w = 0$ on ∂O, and

$$\mu(w,v) := \int_\Omega (A\nabla w\cdot\nabla\bar v - bk^2 w\bar v)\mathrm{d}\boldsymbol{x} = 0 \qquad \forall\, v \in H_0^1(\Omega). \tag{16}$$

Let $\mathcal{M}_h$ be a regular conforming partition of Ω such that each element in $\mathcal{M}_h$ is a tetrahedron. Let $V_h \subset H^1(\Omega)$ be the conforming linear finite element space over Ω. Since $\mathcal{M}_h$ yields a regular triangulation of ∂S, $V_h|_{\partial S}$ also defines a continuous linear finite element space on ∂S. Let $f_h := \Pi_h f_S \in V_h|_{\partial S}$ be a finite element approximation of f_S, where Π_h is chosen as the nodal interpolation operator if $f_S \in C^0(\partial S)$ and as the quasi-interpolation operator using local regularization [22, 23] if $f_S \notin C^0(\partial S)$. The finite element approximation to the PML problem (16) is: Find $w_h \in V_h$ such that $w_h = f_h$ on ∂S, $w_h = 0$ on ∂O, and

$$\mu(w_h, v) = 0 \qquad \forall\, v \in V_h \cap H_0^1(\Omega). \tag{17}$$

Following the general theory in [24, Chapter 5], the existence of unique solution of the discrete problem (17) and the finite element convergence analysis depend on the following discrete inf-sup condition

$$\sup_{0\neq v\in V_h\cap H_0^1(\Omega)} \frac{|\mu(\psi_h, v)|}{\|v\|_{H^1(\Omega)}} \geq C\|\psi_h\|_{H^1(\Omega)} \qquad \forall\, \psi_h \in V_h \cap H_0^1(\Omega). \tag{18}$$

where the constant $C > 0$ is independent of the mesh size. Since the continuous problem (16) has a unique solution by Theorem 3.2, the sesquilinear form μ: $H_0^1(\Omega)\times H_0^1(\Omega)$ satisfies the continuous inf-sup condition. It is well-known that $V_h \cap H_0^1(\Omega)$ is dense in $H_0^1(\Omega)$ as the mesh size $h \to 0$. Using a general argument of Schatz [25], (18) holds when the mesh size is sufficiently small, i.e., $h \ll 1$.

To derive the a posteriori error estimates for (17), we introduce

$$\begin{aligned} R_K &:= \nabla\cdot\Big(A\nabla(w_h|_K)\Big) + bk^2(w_h|_K) \qquad \text{in } K \in \mathcal{M}_h, \\ J_F &:= \Big[(A\nabla w_h)\cdot \boldsymbol{n}_F\Big]_F \qquad \text{on any interior face } F \text{ of } \mathcal{M}_h, \end{aligned}$$

where $[v]_F := v|_{K_1} - v|_{K_2}$ on F for any $F = K_1 \cap K_2$, $K_1, K_2 \in \mathcal{M}_h$. Here $\boldsymbol{n}_F$ is the unit normal to face F, R_K stands for the element residual of the discrete equation, and J_F stands for the jump of the normal flux on face F. For any $K \in \mathcal{M}_h$, the local error indicator η_K is defined as

$$\eta_K^2 = \|h_K R_K\|^2_{L^2(K)} + \frac{1}{2}\sum_{F\subset\partial K\setminus(\partial S\cup\partial B)} h_F\|J_F\|^2_{L^2(F)},$$

where h_K, h_F are the diameters of K, F respectively. Using similar arguments as in [12, Section 4], we obtain the upper bound estimate of the a posteriori error estimate.

Theorem 3.3. *Let* (H1)–(H2) *be satisfied and $\bar\sigma$ be large enough. There exists a constant C which depends on k and $\bar\sigma$ at most polynomially such that*

$$\begin{aligned} \|\hat w - w_h\|_{H^1(B\setminus\overline{S})} \le C\Big\{ &\|f_S - f_h\|_{H^{1/2}(\partial S)} + \alpha_0^2(1+kL)\Big(\sum_{K\in\mathcal{M}_h}\eta_K^2\Big)^{1/2} \\ &+ \alpha_0^3(1+kL)^3 e^{-\gamma k\bar\sigma}\,\|w_h\|_{H^{1/2}(\partial B)}\Big\}. \end{aligned}$$

4. Multiple scattering problems

In Section 3, we have studied the UPML approximation and finite element approximation to each single scattering problem in (5). In this section, we shall adopt the theories to the whole system.

Denote $R_i = \mathrm{diam}(D_i)/2$ and let $\boldsymbol{c}_i = (c_{i,1}, c_{i,2}, c_{i,3}) \in \mathbb{R}^3$ satisfy $D_i \subset B(\boldsymbol{c}_i, R_i)$. We define the truncated domains $B_i \supset \overline{D}_i$ as follows

$$B_i = \{(x_1,x_2,x_3) : |x_m - c_{i,m}| < L_{i,m},\ m = 1,2,3\} \qquad 1 \le i \le I. \tag{19}$$

For convenience and without loss of generality, we assume $2R_i < L_{i,m} < 4R_i$, $m = 1,2,3$ which means that we are only interested in the scattering field in the neighborhood of D. Since $D_1,\cdots,D_I$ are well-separated, we also assume that $B_i \cap B_j = \emptyset$ for any $1 \le i < j \le I$.

Let $\chi_i(\boldsymbol{x}) = \chi(\frac{\boldsymbol{x}-\boldsymbol{c}_i}{R_i})$, $1 \le i \le I$, be cutoff functions, where

$$\chi(\boldsymbol{x}) = \begin{cases} 1, & \text{if } |\boldsymbol{x}| \le 1, \\ [1+\cos(\pi|\boldsymbol{x}| - \pi)]/2, & \text{if } 1 < |\boldsymbol{x}| < 2, \\ 0, & \text{if } |\boldsymbol{x}| \ge 2. \end{cases} \tag{20}$$

Clearly $\chi_i \in C^1(\mathbb{R}^3)$, $\mathrm{supp}(\chi_i) \subset B_i$, and $\|\nabla\chi_i\|_{0,\infty,\mathbb{R}^3} \leq 2/R_i$. We introduce the wave propagation operators as follows

$$P_i(v) = \int_{B_i\setminus\overline{D}_i} \Big(\nabla_{\boldsymbol{y}} G(\cdot,\boldsymbol{y})v(\boldsymbol{y}) - \nabla v(\boldsymbol{y})G(\cdot,\boldsymbol{y})\Big) \cdot \nabla\chi_i(\boldsymbol{y})\mathrm{d}\boldsymbol{y} \quad \text{in } \mathbb{R}^3 \setminus \overline{B}_i, \tag{21}$$

for any $v \in H^1(B_i \setminus \overline{D}_i)$ and $1 \leq i \leq I$. Since $\chi_j \equiv 1$ on ∂D_j, from (2), (5), and the formula of integration by parts, we deduce that

$$P_i(u_i) = u_i \quad \text{in } \mathbb{R}^3 \setminus \overline{B}_i, \quad 1 \leq i \leq I. \tag{22}$$

The following lemma is an easy result of (21) and the estimation for the fundamental solution.

Lemma 4.1. *There exists a constant $C_{k,R_{\max}}$ only depending on k, $R_{\max}$ such that*

$$\|P_i(v)\|_{1,\infty,B_j} \leq C_{k,R_{\max}} d_{\min}^{-1} \|v\|_{H^1(B_i\setminus\overline{D}_i)} \qquad \forall\, j \neq i,\ v \in H^1(B_i \setminus \overline{D}_i),$$

where $d_{\min} := \min\limits_{1\leq i<j\leq I} \mathrm{dist}(B_i, B_j)$ *and* $R_{\max} := \max\limits_{1\leq i\leq I} R_i$.

A weak formulation of (5) is: Find $u_i \in H^1(B_i \setminus \overline{D}_i)$ such that $u_i = g - \sum_{j=1,j\neq i}^{I} P_j(u_j)$ on Γ_i and

$$a_i(u_i, v) = 0 \qquad \forall\, v \in H^1_{\Gamma_i}(B_i \setminus \overline{D}_i), \tag{23}$$

where the sesquilinear a_i is defined by

$$a_i(\psi,\phi) := \int_{B_i\setminus\overline{D}_i} \left(\nabla\psi \cdot \nabla\bar{\phi} - k^2\psi\bar{\phi}\right) \mathrm{d}\boldsymbol{x} - \langle T_i\psi, \phi\rangle_{\partial B_i} \qquad \forall\, \psi,\phi \in H^1(B_i \setminus \overline{D}_i).$$

The DtN operator T_i is defined as follows: Given $f_i \in H^{1/2}(\partial B_i)$, $T_i f_i = \frac{\partial\xi_i}{\partial\boldsymbol{n}}$ on ∂B_i, where ξ_i solves the following scattering problem

$$\begin{cases} \Delta\xi_i + k^2\xi_i = 0 & \text{in } \mathbb{R}^3 \setminus \overline{B}_i, \\ \xi_i = f_i & \text{on } \partial B_i, \qquad\qquad 1 \leq i \leq I. \\ \lim_{r\to\infty} r\left|\frac{\partial\xi_i}{\partial r} - \mathbf{i}k\xi_i\right| = 0, & \end{cases} \tag{24}$$

It is well-known that the scattering problem (23) has a unique solution $u_i \in H^1_{\Gamma_i}(B_i\setminus\overline{D}_i)$ for any given boundary condition $u_i|_{\Gamma_i} \in H^{1/2}(\Gamma_i)$ (cf. e.g. [16]). This implies that the following inf-sup conditions hold with a constant $C_{\mathrm{IS}} > 0$

$$\sup_{0\neq\psi\in H^1_{\Gamma_i}(B_i\setminus\overline{D}_i)} \frac{|a_i(\phi,\psi)|}{\|\psi\|_{H^1(B_i\setminus\overline{D}_i)}} \geq C_{\mathrm{IS}} \|\phi\|_{H^1(B_i\setminus\overline{D}_i)} \qquad \forall\, \phi \in H^1_{\Gamma_i}(B_i \setminus \overline{D}_i),\ \ 1 \leq i \leq I. \tag{25}$$

4.1. UPML method for multiple scattering problems

We introduce the truncated domains for the PML as follows

$$O_i = \left\{(x_1, x_2, x_3) : |x_m - c_{i,m}| \leq L_{i,m} + d_m,\ m = 1, 2, 3\right\}, \quad 1 \leq i \leq I. \tag{26}$$

According to (9), the UPML in O_i is defined by the complex coordinate stretching

$$\widetilde{x}_m = x_m + \mathbf{i} \int_0^{x_m - c_{i,m}} \sigma_{i,m}(t) \mathrm{d}t, \quad 1 \leq m \leq 3, \qquad \forall\, \boldsymbol{x} \in \overline{O}_i, \tag{27}$$

where $\sigma_{i,m}(t) = 0$ if $|t| \leq L_{i,m}$ and $\sigma_{i,m}(t) = \widetilde{\sigma}_m \left(\frac{|t| - L_{i,m}}{d_m}\right)^n$ if $L_{i,m} < |t| \leq L_{i,m} + d_m$. From (H1) we easily know that

$$\int_{L_{i,m}}^{L_{i,m}+d_m} \sigma_{i,m}(t) \mathrm{d}t = \bar{\sigma}, \qquad \forall\, 1 \leq m \leq 3,\ 1 \leq i \leq I.$$

In view of (12), we define the PML approximation to (5) by

$$\begin{cases} \nabla \cdot (A_i \nabla \hat{u}_i) + b_i k^2 \hat{u}_i = 0 & \text{in } \ \Omega_i = O_i \setminus \overline{D}_i, \\ \hat{u}_i = g - \sum_{j=1, j\neq i}^{I} P_j(\hat{u}_j) & \text{on } \ \Gamma_i, \\ \hat{u}_i = 0 & \text{on } \ \partial O_i, \end{cases} \qquad 1 \leq i \leq I, \tag{28}$$

where $A_i = \mathrm{diag}\left(\frac{\alpha_{i,2}\alpha_{i,3}}{\alpha_{i,1}}, \frac{\alpha_{i,1}\alpha_{i,3}}{\alpha_{i,2}}, \frac{\alpha_{i,1}\alpha_{i,2}}{\alpha_{i,3}}\right)$ and $b_i = \alpha_{i,1}\alpha_{i,2}\alpha_{i,3}$ with $\alpha_{i,m} = 1 + \mathbf{i}\sigma_{i,m}$, $1 \leq m \leq 3$.

Theorem 4.2. *Let* (H1)–(H2) *be satisfied and let* $u_i, \hat{u}_i$, $1 \leq i \leq I$ *be the solutions to* (5) *and* (28) *respectively. Suppose* $\bar{\sigma}, d_{\min}$ *are sufficiently large. There exists a constant* C *which depends on* k, $\bar{\sigma}$ *at most polynomially such that*

$$\sum_{i=1}^{I} \|u_i - \hat{u}_i\|_{H^1(B_i \setminus \overline{D}_i)} \leq C\alpha_0^3 (1 + kL)^3 e^{-k\gamma\bar{\sigma}} \sum_{i=1}^{I} \|\hat{u}_i\|_{H^{1/2}(\partial B_i)},$$

where γ, α_0, L *are the constants in Theorem 3.2 and take their largest values among all* $1 \leq i \leq I$ *with* $S = D_i, B = B_i$.

Proof. It is clear that (28) is the PML approximation of the scattering problems

$$\begin{cases} \Delta U_i + k^2 U_i = 0 & \text{in } \ \mathbb{R}^3 \setminus \overline{D}_i, \\ U_i = g - \sum_{j=1, j\neq i}^{I} P_j(\hat{u}_j) & \text{on } \ \Gamma_i, \\ \lim_{r\to\infty} r \left| \frac{\partial U_i}{\partial r} - \mathbf{i}kU_i \right| = 0, \end{cases} \qquad 1 \leq i \leq I. \tag{29}$$

Then Theorem 3.2 yields

$$\|U_i - \hat{u}_i\|_{H^1(B_i \setminus \overline{D}_i)} \leq C\alpha_0^3 (1 + kL)^3 e^{-k\gamma\bar{\sigma}} \|\hat{u}_i\|_{H^{1/2}(\Gamma_i)}. \tag{30}$$

Denote $e_i = u_i - U_i$ and $f_i = \sum_{j=1,j\neq i}^{I} P_j(\hat{u}_j - u_j)$. Subtracting (29) from (5) and using (22), we find that e_i solve the following scattering problems

$$\begin{cases} \Delta e_i + k^2 e_i = 0 & \text{in } \mathbb{R}^3 \setminus \overline{D}_i, \\ e_i = f_i & \text{on } \Gamma_i, \qquad\qquad 1 \leq i \leq I. \\ \lim_{r\to\infty} r\left|\frac{\partial e_i}{\partial r} - \mathbf{i}ke_i\right| = 0, & \end{cases}$$

By the trace theorem, there exists a $\phi_i \in H^1(B_i \setminus \overline{D}_i)$ such that $\phi_i = f_i$ on Γ_i and

$$\|\phi_i\|_{H^1(B_i\setminus\overline{D}_i)} \leq C\|f_i\|_{H^{1/2}(\Gamma_i)} \leq Cd_{\min}^{-1} \sum_{j=1,j\neq i}^{I} \left\|u_j - \hat{u}_j\right\|_{H^1(B_j\setminus\overline{D}_j)},$$

where we have used Lemma 4.1 and the constant C only depends on k and $B_1, \cdots, B_I$. Since e_i satisfies (23), by the inf-sup condition in (25), we have

$$\begin{aligned} \|e_i - \phi_i\|_{H^1(B_i\setminus\overline{D}_i)} &\leq C_{\mathrm{IS}}^{-1} \sup_{0\neq v\in H^1_{\Gamma_i}(B_i\setminus\overline{D}_i)} \frac{a_i(e_i - \phi_i, v)}{\|v\|_{H^1(B_i\setminus\overline{D}_i)}} \\ &= C_{\mathrm{IS}}^{-1} \sup_{0\neq v\in H^1_{\Gamma_i}(B_i\setminus\overline{D}_i)} \frac{a_i(\phi_i, v)}{\|v\|_{H^1(B_i\setminus\overline{D}_i)}} \leq C\|\phi_i\|_{H^1(B_i\setminus\overline{D}_i)}. \end{aligned}$$

Then there exists a constant C only depends on k and $B_1, \cdots, B_I$ such that

$$\|e_i\|_{H^1(B_i\setminus\overline{D}_i)} \leq C_1 d_{\min}^{-1} \sum_{j=1,j\neq i}^{I} \left\|u_j - \hat{u}_j\right\|_{H^1(B_j\setminus\overline{D}_j)}. \tag{31}$$

Combining (30) and (31) leads to

$$\|u_i - \hat{u}_i\|_{H^1(B_i\setminus\overline{D}_i)} \leq C\alpha_0^3(1+kL)^3 e^{-k\gamma\bar{\sigma}} \|\hat{u}_i\|_{H^{1/2}(\Gamma_i)} + C_1 d_{\min}^{-1} \sum_{j=1,j\neq i}^{I} \left\|u_j - \hat{u}_j\right\|_{H^1(B_j\setminus\overline{D}_j)}.$$

Summing up the above inequality in i yields

$$\sum_{i=1}^{I} \|u_i - \hat{u}_i\|_{H^1(B_i\setminus\overline{D}_i)} \leq C\alpha_0^3(1+kL)^3 e^{-k\gamma\bar{\sigma}} \sum_{i=1}^{I} \|\hat{u}_i\|_{H^{1/2}(\Gamma_i)} + C_1 I d_{\min}^{-1} \sum_{i=1}^{I} \left\|u_j - \hat{u}_j\right\|_{H^1(B_j\setminus\overline{D}_j)}.$$

Notice that $d_{\min}$ is large enough and the constant C_1 only depends on k and $B_1, \cdots, B_I$. We complete the proof by letting $d_{\min} \geq 2C_1 I$. □

4.2. A posteriori error estimate for multiple scattering problems

Let $\mathcal{M}_i$ be the regular conforming trangulation of Ω_i and $V_i \subset H^1(\Omega_i)$ be the conforming linear finite element space over $\mathcal{M}_i$. We denote by Π_i: $C^0(\overline{\Omega}_i) \mapsto V_i$ the nodal interpolation operator of the linear Lagrangian finite elements on $\mathcal{M}_i$ for $1 \leq i \leq I$.

From (17), the finite element approximation to the PML problem (28) is: Find $u_i^h \in V_i$ such that $u_i^h = f_i^h$ on Γ_i, $u_i^h = 0$ on ∂O_i, and

$$\mu_i(u_i^h, v) := \int_{\Omega_i} (A_i \nabla u_i^h \cdot \nabla \bar{v} - b_i k^2 u_i^h \bar{v}) \mathrm{d}\boldsymbol{x} = 0 \quad \forall\, v \in V_i \cap H_0^1(\Omega_i),\ 1 \le i \le I, \tag{32}$$

where $f_i^h = g_h - \Pi_i \sum_{j=1,j\neq i}^I P_j(u_j^h)$ and g_h is some finite element approximation of g satisfying $g_h|_{\Gamma_i} \in V_i|_{\Gamma_i}$. Clearly (32) is a system of discrete equations coupled by the boundary conditions. It is just the wave propagation operators $P_1, \cdots, P_I$ that produces dense blocks in the global stiffness matrix.

For any $1 \le i \le I$ and any $K \in \mathcal{M}_i$, the local error indicator η_K is defined as

$$\eta_K^2 = \|h_K R_K\|_{L^2(K)}^2 + \frac{1}{2} \sum_{F \subset \partial K \backslash \partial S} h_F \|J_F\|_{L^2(F)}^2, \tag{33}$$

where $R_K := \nabla \cdot \left(A \nabla (u_i^h|_K)\right) + bk^2 (u_i^h|_K)$ in any $K \in \mathcal{M}_i$ and $J_F := \left[(A\nabla u_i^h)\cdot \boldsymbol{n}_F\right]_F$ on any interior face F of $\mathcal{M}_i$.

Theorem 4.3. *Let* (H1)–(H2) *be satisfied and let $\bar{\sigma}, d_{\min}$ be large enough. Then*

$$\begin{aligned}\sum_{i=1}^I \left\|u_i - u_i^h\right\|_{H^1(B_i\backslash \overline{D}_i)} \le & C \sum_{i=1}^I \Big\{ \Big\| g - \sum_{j=1,j\neq i}^I P_j(u_j^h) - f_i^h \Big\|_{H^{1/2}(\Gamma_i)} \\ & + \alpha_0^2 (1+kL) \Big(\sum_{K\in\mathcal{M}_i} \eta_K^2 \Big)^{\frac{1}{2}} + \alpha_0^3 (1+kL)^3 e^{-\gamma k \bar{\sigma}} \left\|u_i^h\right\|_{H^{\frac{1}{2}}(\partial B_i)} \Big\},\end{aligned}$$

where the constants C, α_0, γ, L are same to those in Theorem 4.2.

Proof. An application of Theorem 3.3 shows that

$$\begin{aligned}\left\|\hat{u}_i - u_i^h\right\|_{H^1(B_i\backslash \overline{D}_i)} \le & C \Big\{ \Big\| g - \sum_{j=1,j\neq i}^I P_j(u_j^h) - f_i^h \Big\|_{H^{1/2}(\Gamma_i)} + \Big\| \sum_{j=1,j\neq i}^I P_j(\hat{u}_j - u_j^h) \Big\|_{H^{1/2}(\Gamma_i)} \\ & + \alpha_0^2 (1+kL) \Big(\sum_{K\in\mathcal{M}_i} \eta_K^2 \Big)^{1/2} + \alpha_0^3 (1+kL)^3 e^{-\gamma k \bar{\sigma}} \left\|u_i^h\right\|_{H^{1/2}(\partial B_i)} \Big\}.\end{aligned} \tag{34}$$

From Lemma 4.1, there exists a constant C_1 only depending on k and $B_1, \cdots, B_I$ such that

$$\Big\| \sum_{j=1,j\neq i}^I P_j(\hat{u}_j - u_j^h) \Big\|_{H^{\frac{1}{2}}(\Gamma_i)} \le C_1 d_{\min}^{-1} \sum_{j=1,j\neq i}^I \left\|\hat{u}_j - u_j^h\right\|_{H^1(B_j\backslash \overline{D}_j)}.$$

Now we insert this inequality into (34) and sum up (34) in $1 \le i \le I$. Then letting $d_{\min} \ge 2IC_1$ yields

$$\begin{aligned}\sum_{i=1}^I \left\|\hat{u}_i - u_i^h\right\|_{H^1(B_i\backslash \overline{D}_i)} \le & C \sum_{i=1}^I \Big\{ \Big\| g - \sum_{j=1,j\neq i}^I P_j(u_j^h) - f_i^h \Big\|_{H^{1/2}(\Gamma_i)} \\ & + \alpha_0^2 (1+kL) \Big(\sum_{K\in\mathcal{M}_i} \eta_K^2 \Big)^{\frac{1}{2}} + \alpha_0^3 (1+kL)^3 e^{-\gamma k \bar{\sigma}} \left\|u_i^h\right\|_{H^{1/2}(\partial B_i)} \Big\}.\end{aligned}$$

From Theorem 4.2 we know that

$$\begin{aligned}\sum_{i=1}^{I}\|u_i-\hat{u}_i\|_{H^1(B_i\backslash\overline{D}_i)} \leq & C\alpha_0^3(1+kL)^3e^{-k\gamma\bar{\sigma}}\sum_{i=1}^{I}\|\hat{u}_i\|_{H^{1/2}(\partial B_i)} \\ & \leq C\alpha_0^3(1+kL)^3e^{-k\gamma\bar{\sigma}}\sum_{i=1}^{I}\left\{\left\|\hat{u}_i-u_i^h\right\|_{H^1(B_i\backslash\overline{D}_i)}+\left\|u_i^h\right\|_{H^{1/2}(\partial B_i)}\right\}.\end{aligned}$$

The proof is completed upon summing up the above two inequalities and letting $C\alpha_0^3(1+kL)^3e^{-k\gamma\bar{\sigma}}<1/2$. □

5. Alternative iteration method

As remarked previously, (32) is a coupled system of discrete problems. The wave propagation operators $P_1,\cdots,P_I$ yield dense blocks in the global stiffness matrix and make the algebraic system hard to solve. We shall propose an efficient method for the solution of (32) and derive the a posteriori error estimate.

5.1. Block Gauss-Seidel method

For any $1\leq i\leq I$, we denote by $\mathcal{V}_i$ the set of vertices of $\mathcal{M}_i$ which are not on ∂O_i and let $b_{\mathbf{v}}\in V_i$ be the nodal basis function belonging to vertex $\mathbf{v}\in\mathcal{V}_i$. Then the solution of (32) is represented as $u_i^h=\sum_{\mathbf{v}\in\mathcal{V}_i}u_i^h(\mathbf{v})b_{\mathbf{v}}$. The discrete problem (32) is equivalent to the following system of algebraic equations

$$\begin{pmatrix}\mathbb{A}_1 & \mathbb{P}_{1,2} & \cdots & \mathbb{P}_{1,I}\\ \mathbb{P}_{2,1} & \mathbb{A}_2 & \cdots & \mathbb{P}_{2,I}\\ \vdots & \vdots & \cdots & \vdots\\ \mathbb{P}_{I,1} & \mathbb{P}_{I,2} & \cdots & \mathbb{A}_I\end{pmatrix}\begin{pmatrix}\mathbb{U}_1\\ \mathbb{U}_2\\ \vdots\\ \mathbb{U}_I\end{pmatrix}=\begin{pmatrix}\mathbb{G}_1\\ \mathbb{G}_2\\ \vdots\\ \mathbb{G}_I\end{pmatrix}, \tag{35}$$

where each $\mathbb{U}_i$ is an unknown vector whose entries are $\mathbb{U}_{i;\mathbf{v}}=u_i^h(\mathbf{v})$ for all $\mathbf{v}\in\mathcal{V}_i$, $\mathbb{A}_i$ is the stiffness matrix for the discrete problem of u_i^h and its entries are defined by

$$\begin{aligned}\mathbb{A}_{i;\mathbf{v},\mathbf{v}'} &= \mu_i(b_{\mathbf{v}},b_{\mathbf{v}'}) && \forall\,\mathbf{v}\in\mathcal{V}_i\backslash\Gamma_i \text{ and } \mathbf{v}'\in\mathcal{V}_i,\\ \mathbb{A}_{i;\mathbf{v},\mathbf{v}'} &= \delta_{\mathbf{v},\mathbf{v}'} && \forall\,\mathbf{v}\in\mathcal{V}_i\cap\Gamma_i \text{ and } \mathbf{v}'\in\mathcal{V}_i,\end{aligned}$$

$\mathbb{P}_{i,j}$, $i\neq j$, are the propagation matrices with the entries

$$\begin{aligned}\mathbb{P}_{i,j;\mathbf{v},\mathbf{v}'} &= 0 && \forall\,\mathbf{v}\in\mathcal{V}_i\backslash\Gamma_i \text{ and } \mathbf{v}'\in\mathcal{V}_j,\\ \mathbb{P}_{i,j;\mathbf{v},\mathbf{v}'} &= \big(P_j(b_{\mathbf{v}'})\big)(\mathbf{v}) && \forall\,\mathbf{v}\in\mathcal{V}_i\cap\Gamma_i \text{ and } \mathbf{v}'\in\mathcal{V}_j,\end{aligned}$$

and the entries of each vector $\mathbb{G}_i$ are given by

$$\mathbb{G}_{i;\mathbf{v}}=0\quad\forall\,\mathbf{v}\in\mathcal{V}_i\backslash\Gamma_i\qquad\text{and}\qquad\mathbb{G}_{i;\mathbf{v}}=g_h(\mathbf{v})\quad\forall\,\mathbf{v}\in\mathcal{V}_i\cap\Gamma_i.$$

A block Gauss-Seidel method for the solution of (35) reads: Given $\mathbb{U}_1^{(0)}, \cdots, \mathbb{U}_I^{(0)}$, define $\mathbb{U}_1^{(n)}, \cdots, \mathbb{U}_I^{(n)}$, $n \geq 1$ by the solution of the following system of equations

$$\mathbb{A}_i \mathbb{U}_i^{(n)} = \mathbb{G}_i - \sum_{j=1}^{i-1} \mathbb{P}_{i,j} \mathbb{U}_j^{(n)} - \sum_{j=i+1}^{I} \mathbb{P}_{i,j} \mathbb{U}_j^{(n-1)}, \qquad 1 \leq i \leq I. \tag{36}$$

Write

$$u_i^{n,h} = \sum_{\mathbf{v} \in \mathcal{V}_i} \mathbb{U}_{i;\mathbf{v}}^{(n)} b_{\mathbf{v}}, \qquad n \geq 0.$$

Clearly (36) is equivalent to the discrete weak formulation: Given $\left(u_1^{0,h}, \cdots, u_I^{0,h}\right)$, find $u_i^{n,h} \in V_i$ such that $u_i^{n,h} = f_i^{n,h}$ on Γ_i, $u_i^{n,h} = 0$ on ∂O_i, and

$$\mu_i(u_i^{n,h}, v) := \int_{\Omega_i} (A_i \nabla u_i^{n,h} \cdot \nabla \bar{v} - b_i k^2 u_i^{n,h} \bar{v}) \mathrm{d}\boldsymbol{x} = 0 \quad \forall\, v \in V_i \cap H_0^1(\Omega_i), \tag{37}$$

where

$$f_i^{n,h} = g_h - \Pi_i \sum_{j=1}^{i-1} P_j(u_j^{n,h}) - \Pi_i \sum_{j=i+1}^{I} P_j(u_j^{n-1,h}), \qquad 1 \leq i \leq I.$$

Clearly (37) is an alternative iteration scheme of (32).

5.2. *An alternative iteration method for* (28)

First we study an alternative iteration method for the continuous PML problem (28) :

$$\begin{cases} \nabla \cdot (A_i \nabla \hat{u}_i^{(n)}) + b_i k^2 \hat{u}_i^{(n)} = 0 & \text{in } \Omega_i, \\ \hat{u}_i^{(n)} = g - \sum_{j=1}^{i-1} P_j(\hat{u}_j^{(n)}) - \sum_{j=i+1}^{I} P_j(\hat{u}_j^{(n-1)}) & \text{on } \Gamma_i, \qquad 1 \leq i \leq I, \\ \hat{u}_i^{(n)} = 0 & \text{on } \partial O_i, \end{cases} \tag{38}$$

where $n \geq 1$ and $\hat{u}_1^{(0)}, \cdots, \hat{u}_I^{(0)}$ are given. By Theorem 3.2, (38) has a unique solution for each $1 \leq i \leq I$. It is easy to see that (37) is an finite element approximation to (38).

Theorem 5.1. *Let* (H1)–(H2) *be satisfied and let* $u_i, \hat{u}_i^{(n)}$, $1 \leq i \leq I$ *be the solutions to* (5) *and* (38) *respectively. Suppose* $\bar{\sigma}, d_{\min}$ *are large enough. Then*

$$\sum_{i=1}^{I} \left\| u_i - \hat{u}_i^{(n)} \right\|_{H^1(B_i \setminus \overline{D}_i)} \leq C \alpha_0^3 (1+kL)^3 e^{-k\gamma\bar{\sigma}} \sum_{i=1}^{I} \|\hat{u}_i\|_{H^{1/2}(\partial B_i)} + C_1 d_{\min}^{-1} \sum_{i=1}^{I} \left\| u_i - \hat{u}_i^{(n-1)} \right\|_{H^1(B_i \setminus \overline{D}_i)}, \tag{39}$$

where C, γ, α_0, L *are same to those in Theorem 4.2 and the constant* C_1 *only depends on* k *and* $B_1, \cdots, B_I$.

Proof. It is clear that (38) is the PML approximation to the scattering problems

$$\begin{cases} \Delta U_i + k^2 U_i = 0 & \text{in } \mathbb{R}^3 \setminus \overline{D}_i, \\ U_i = g - \sum_{j=1}^{i-1} P_j(\hat{u}_j^{(n)}) - \sum_{j=i+1}^{I} P_j(\hat{u}_j^{(n-1)}) & \text{on } \Gamma_i, \\ \lim_{r\to\infty} r\left|\frac{\partial U_i}{\partial r} - \mathbf{i}kU_i\right| = 0, \end{cases} \qquad 1 \le i \le I. \tag{40}$$

Then Theorem 3.2 yields

$$\left\|U_i - \hat{u}_i^{(n)}\right\|_{H^1(B_i\setminus\overline{D}_i)} \le C\alpha_0^3(1+kL)^3 e^{-k\gamma\bar{\sigma}} \left\|\hat{u}_i^{(n)}\right\|_{H^{1/2}(\Gamma_i)}. \tag{41}$$

Define $e_i = u_i - U_i$ and $f_i = \sum_{j=1}^{i-1} P_j\left(\hat{u}_j^{(n)} - u_j\right) + \sum_{j=i+1}^{I} P_j\left(\hat{u}_j^{(n-1)} - u_j\right)$. Subtracting (40) from (5) and using (22), we find that e_i satisfies

$$\begin{cases} \Delta e_i + k^2 e_i = 0 & \text{in } \mathbb{R}^3 \setminus \overline{D}_i, \\ e_i = f_i & \text{on } \Gamma_i, \\ \lim_{r\to\infty} r\left|\frac{\partial e_i}{\partial r} - \mathbf{i}ke_i\right| = 0, \end{cases} \qquad 1 \le i \le I.$$

Using similar arguments as in the proof of Theorem 4.2, we obtain

$$\|e_i\|_{H^1(B_i\setminus\overline{D}_i)} \le \frac{C}{d_{\min}}\left\{\sum_{j=1}^{i-1}\left\|u_j - \hat{u}_j^{(n)}\right\|_{H^1(B_j\setminus\overline{D}_j)} + \sum_{j=i+1}^{I}\left\|u_j - \hat{u}_j^{(n-1)}\right\|_{H^1(B_j\setminus\overline{D}_j)}\right\}.$$

Combining the above inequality with (41) and summing them up in i, we have

$$\begin{aligned} \sum_{i=1}^{I}\left\|u_i - \hat{u}_i^{(n)}\right\|_{H^1(B_i\setminus\overline{D}_i)} \le & C\alpha_0^3(1+kL)^3 e^{-k\gamma\bar{\sigma}} \sum_{i=1}^{I}\left\|\hat{u}_i^{(n)}\right\|_{H^{1/2}(\Gamma_i)} \\ & + C_1 I d_{\min}^{-1} \sum_{i=1}^{I}\left\{\left\|u_i - \hat{u}_i^{(n)}\right\|_{H^1(B_i\setminus\overline{D}_i)} + \left\|u_i - \hat{u}_i^{(n-1)}\right\|_{H^1(B_i\setminus\overline{D}_i)}\right\}. \end{aligned}$$

Notice that $d_{\min}$ is large enough and the constant C_1 only depends on k and $B_1, \cdots, B_I$. We complete the proof by letting $d_{\min} \ge 2C_1 I$. $\square$

Remark 5.2. If we choose $\bar{\sigma}$ so large that the first term on the righthand side of (39) is negligible, then the iteration error $E_n := \sum_{i=1}^{I}\left\|u_i - \hat{u}_i^{(n)}\right\|_{H^1(B_i\setminus\overline{D}_i)}$ satisfies

$$E_n \le C_1 d_{\min}^{-1} E_{n-1} \le \cdots \le \left(C_1 d_{\min}^{-1}\right)^n E_0. \tag{42}$$

Since the sub-scatterers are well-separated, (42) yields the exponential convergence of the alternative iteration method for $0 < C_1 d_{\min}^{-1} < 1$.

For any $K \in \cup_{i=1}^{I}\mathcal{M}_i$, let η_K be the local error indicators in (33) with u_i^h replaced by $u_i^{n,h}$. By Theorem 3.3 and Lemma 4.1, we easily get the theorem on the a posteriori error estimate of $u_i^{n,h}$.

Theorem 5.3. *Let* (H1)–(H2) *be satisfied and let* $\bar{\sigma}, d_{\min}$ *be large enough. Then*

$$\left\|\hat{u}_i^{(n)} - u_i^{n,h}\right\|_{H^1(B_i\setminus\overline{D}_i)} \leq C\eta_n + C_1 d_{\min}^{-1} \sum_{j=i+1}^{I} \left\|\hat{u}_j^{(n-1)} - u_j^{n-1,h}\right\|_{H^1(B_j\setminus\overline{D}_j)},$$

where C, C_1 *are the constants in Theorem 5.1 and the a posteriori error estimate is defined by*

$$\eta_n := \left\|f_i^n - f_i^{n,h}\right\|_{H^{\frac{1}{2}}(\Gamma_i)} + \alpha_0^2(1+kL)\Big(\sum_{K\in\mathcal{M}_i} \eta_K^2\Big)^{\frac{1}{2}} + \alpha_0^3(1+kL)^3 e^{-\gamma k\bar{\sigma}} \left\|u_i^{n,h}\right\|_{H^{\frac{1}{2}}(\partial B_i)},$$

$$f_i^n := g - \sum_{j=1}^{i-1} P_j(u_j^{n,h}) - \sum_{j=i+1}^{I} P_j(u_j^{n-1,h}).$$

Remark 5.4. As $n \to \infty$, Theorem 5.3 indicates that $\left\|\hat{u}_i^{(n)} - u_i^{n,h}\right\|_{H^1(B_i\setminus\overline{D}_i)}$ is mainly bounded by the a posteriori error estimate η_n, and Theorem 5.1 indicates that η_n also provides an upper bound for $\left\|u_i - u_i^{n,h}\right\|_{H^1(B_i\setminus\overline{D}_i)}$. Our numerical experiments show that $d_{\min}^{-1} \sum_{j=2}^{I} \left\|u_j - u_j^{n-1,h}\right\|_{H^1(B_j\setminus\overline{D}_j)}$ becomes very small after a few iterations (e.g., $n = 3$) if $d_{\min} \gg R_{\max}$ (see Lemma 4.1).

6. Adaptive UPML algorithms and numerical experiments

In this section, we propose two adaptive UPML algorithms, i.e. APML and AAPML, and demonstrate the efficiency of AAPML by some numerical experiments. The implementation of our algorithms is based on the adaptive finite element package PHG (Parallel Hierarchical Grid [26, 27]).

6.1. Adaptive UPML algorithms

We denote the mesh for the computational domain by $\mathcal{M}_h = \cup_{i=1}^{I}\mathcal{M}_i$. Let $\omega = \alpha_0^3(1+kL)^3 e^{-\gamma k\bar{\sigma}}$ be the PML reduction factor and let $\eta_h := \left(\sum_{K\in\mathcal{M}_h} \bar{\eta}_K^2\right)^{1/2}$ be the a posteriori error estimate with

$$\bar{\eta}_K := \sum_{F\subset\partial K\cap\Gamma_i} h_F^{\frac{1}{2}} \Big\|g_h - \sum_{j\neq i} P_j(u_j^h)\Big\|_{H^1(F)} + \alpha_0^2(1+kL)\eta_K \qquad \forall\, K \in \mathcal{M}_i,\ 1 \leq i \leq I. \tag{43}$$

Now we propose the adaptive PML (APML) algorithm for solving (32).

Algorithm 6.1. (APML)

Given the tolerance $\varepsilon > 0$.

1. Fix the truncated domains B_i by choosing $L_{i,1}, L_{i,2}, L_{i,3},\ 1 \leq i \leq I$.
2. Set the PML absorbing layers by choosing d_1, d_2, d_3 and the medium properties such that (H2) is satisfied and $\omega < 10^{-8}$.
3. Construct an initial triangulation $\mathcal{M}_i$ for each $\Omega_i := O_i \setminus \overline{D}_i,\ 1 \leq i \leq I$ and set the error estimate by $\eta_h = 1$.
4. While $\eta_h > \varepsilon$ do

- refine $\mathcal{M}_h$ according to the GERS strategy (cf. e.g. [28]) :

  If $\left(\sum_{K\in\mathcal{M}_h^r}\bar{\eta}_K^2\right)^{1/2} > \theta\eta_h$, refine all elements in $\mathcal{M}_h^r$, where $0 < \theta < 1$ and $\mathcal{M}_h^r$ is the smallest subset of $\mathcal{M}_h$ satisfying the above inequality.
- solve (32) on the new $\mathcal{M}_h$;
- compute $\bar{\eta}_K$ for all $K \in \mathcal{M}_h$ and η_h using the new solution of (32).

end while

To solve (37) or (35), we define the a posteriori error estimate $\hat{\eta}_K$ as follows:

$$\hat{\eta}_K := \sum_{F\subset\partial K\cap\Gamma_i} h_F^{\frac{1}{2}}\left\|g_h - \sum_{j=1}^{i-1} P_j(u_j^h) - \sum_{j=i+1}^{I} P_j(u_j^H)\right\|_{H^1(F)} + \alpha_0^2(1+kL)\eta_K \quad \forall\, K\in\mathcal{M}_i, 1\le i\le I. \tag{44}$$

Here u_i^h is the solution on the newly refined mesh and u_i^H is the solution on the coarse mesh. Let $\hat{\eta}_h := \left(\sum_{K\in\mathcal{M}_h}\hat{\eta}_K^2\right)^{1/2}$. Now we propose the alternative APML (AAPML) algorithm for solving (37) or (35).

Algorithm 6.2. (AAPML)

Given the tolerance $\varepsilon > 0$.

1. Fix the truncated domains B_i by choosing $L_{i,1}, L_{i,2}, L_{i,3}$, $1 \le i \le I$.
2. Set the PML absorbing layers by choosing d_1, d_2, d_3 and the medium properties such that (H2) is satisfied and $\omega < 10^{-8}$.
3. Construct an initial triangulation $\mathcal{M}_i$ for each Ω_i, $1 \le i \le I$.
4. Solve (32) for $u_1^h, \cdots, u_I^h$ on the coarse mesh $\mathcal{M}_h$ and compute the error indicators $\hat{\eta}_K = \bar{\eta}_K$, $K \in \mathcal{M}_h$ by (43). Set $\hat{\eta}_h = \left(\sum_{K\in\mathcal{M}_h}\hat{\eta}_K^2\right)^{1/2}$.
5. While $\hat{\eta}_h > \varepsilon$ do
   - set $u_i^H := u_i^h$ for all $1 \le i \le I$;
   - refine $\mathcal{M}_h$ according to the GERS strategy using $\hat{\eta}_h$ and $\{\hat{\eta}_K : K \in \mathcal{M}_h\}$;
   - on the new $\mathcal{M}_h$, solve (37) for the new solution u_i^h with the boundary conditions $u_i^h = 0$ on ∂O_i and

$$u_i^h = g_h - \sum_{j=1}^{i-1} P_j(u_j^h) - \sum_{j=i+1}^{I} P_j(u_j^H) \quad \text{on } \Gamma_i, \quad 1 \le i \le I;$$

   - compute $\hat{\eta}_K$, $K \in \mathcal{M}_h$ and $\hat{\eta}_h$ by (44) and using u_i^h, u_i^H, $1 \le i \le I$.

   end while

By Algorithm 6.2, the coupled system (32) is only solved on the initial mesh which is very coarse (see Step 4). After that, we only solve one single scattering problem by (37) on each refined mesh $\mathcal{M}_i$. It is clear that Algorithm 6.2 provides an economic and efficient approach for the solution of multiple scattering problems.

6.2. Numerical experiments

Now we report two numerical examples to demonstrate the efficiency of the AAPML algorithm. We set the wave number by $k = 5$, set the PML parameters by $\widetilde{\sigma}_1 = \widetilde{\sigma}_2 = \widetilde{\sigma}_3 = 7$, $n = 0$ in (27), and set $\theta = 0.3$ for the factor in the GERS refinement strategy.

The numerical results are computed by two adaptive PML methods using the second-order Lagrange finite elements: one is the AAPML algorithm (Algorithm 6.2), the other is the adaptive PML method for (1) with global truncations $\overline{D} \subset B \subset O$ (i.e., both B and O are cubic domains). In both cases, we denote by $\mathcal{M}_h$ the partition of the total computational domain, by u_h the finite element approximation to the exact solution u, by η_h the a posteriori error estimate over $\mathcal{M}_h$, and by N_h the number of elements in $\mathcal{M}_h$. Furthermore, we denote by $\Omega = B \setminus \overline{D}$ or $\Omega = \cup_{i=1}^{I}(B_i \setminus \overline{D}_i)$ the domain where the scattering field is desired.

Example 6.1. We consider the double scattering problem with two cubic sub-scatterers $D_1 = (-2.6,\ -2.4) \times (-0.1,\ 0.1) \times (-0.1,\ 0.1)$ and $D_2 = (2.4,\ 2.6) \times (-0.1,\ 0.1) \times (-0.1,\ 0.1)$. The Dirichlet boundary condition on $\partial D_1 \cup \partial D_2$ is set by the exact solution

$$u(\boldsymbol{x}) = \frac{e^{\mathbf{i}kr_1}}{r_1} + \frac{e^{\mathbf{i}kr_2}}{r_2}, \qquad r_1 = |\boldsymbol{x} - \boldsymbol{c}_1|, \quad r_2 = |\boldsymbol{x} - \boldsymbol{c}_2|,$$

where $\boldsymbol{c}_1 = (-2.5, 0, 0)$ and $\boldsymbol{c}_2 = (2.5, 0, 0)$. Clearly u stands for the addition of two point sources located at $\boldsymbol{c}_1, \boldsymbol{c}_2$ respectively. The truncated domains are defined by $L_{1,m} = L_{2,m} = 0.2$ and $d_m = 0.5$ for $m = 1, 2, 3$.

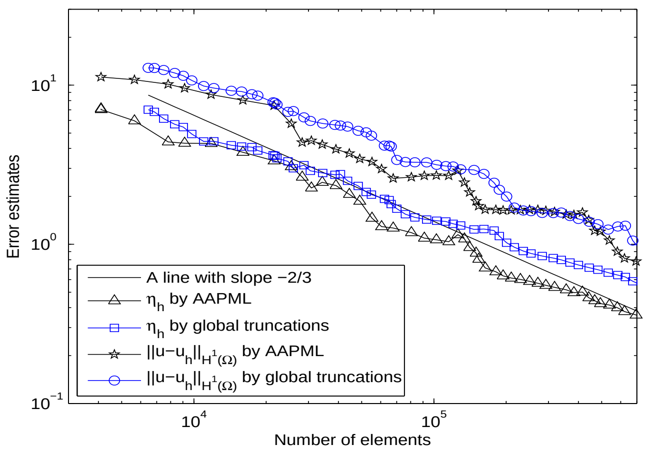

Figure 2: Quasi-optimality of adaptive PML methods for Example 6.1.

In Figure 2, the curve with "circles" and the curve with "stars" show the reduction rate of $\log \|u - u_h\|_{H^1(\Omega)}$ with respect to $\log N_h$, the curve with "squares" and the curve with "triangles" show the reduction rate of $\log \eta_h$ with respect to $\log N_h$. The figure shows that both the AAPML algorithm and the adaptive PML method with global truncations yield quasi-optimal reduction rates: $\|u - u_h\|_{H^1(\Omega)} \sim CN_h^{-2/3}$ and $\eta_h \sim CN_h^{-2/3}$. The initial meshes for the two methods yield approximate error estimates, but have different numbers of elements. During mesh refinements, the difference between the numbers of elements almost keep invariant since the two methods yield similar rates of error reduction. Figure 3 shows the adaptively refined mesh with $224,262$ elements generated by the AAPML algorithm. Figure 4 shows the mesh on a slice of the domain which parallels to the x–z plane. To insure that the reflections from the truncated boundary are negligible, we set the PML reduction factor ω very small in Algorithm 6.1 and 6.2. This results a thick PML compared with the interior domain. However, since the solution decays exponentially in the PML, the mesh becomes much coarse away from the inner boundary.

Figure 3: An adaptive mesh with $224,262$ elements generated by the AAPML algorithm for Example 6.1.

Figure 4: The slice of the mesh in Figure 3 cut by the x–z plane.

One of the important quantities in the scattering problems is the far-field pattern:

$$u_\infty(\widehat{\boldsymbol{x}}) = \frac{1}{4\pi}\int_{\partial D}\left(u(\boldsymbol{y})\frac{\partial e^{-\mathrm{i}k\widehat{\boldsymbol{x}}\cdot\boldsymbol{y}}}{\partial \boldsymbol{n}_{\boldsymbol{y}}} - \frac{\partial u(\boldsymbol{y})}{\partial \boldsymbol{n}}e^{-\mathrm{i}k\widehat{\boldsymbol{x}}\cdot\boldsymbol{y}}\right)\mathrm{d}s_{\boldsymbol{y}},$$

where $\widehat{\boldsymbol{x}} := \boldsymbol{x}/|\boldsymbol{x}| = (\cos\theta\cos\phi, \cos\theta\sin\phi, \sin\theta)$. Figure 5(a) and 5(b) show the far-field pattern $u_\infty(\widehat{\boldsymbol{x}})$ in two observation directions $(\theta,\phi) = (0,\pi/2), (\pi/4,\pi/4)$. Clearly the approximate far-field pattern converges quickly and coincides very well with the exact values as the number of elements increasing.

Example 6.2. This example concerns the scattering of the incident plane wave $u_I = e^{-\mathrm{i}k\,\boldsymbol{d}\cdot\boldsymbol{x}}$ with $\boldsymbol{d} = (1, 1, \sqrt{2})/2$. The Dirichlet boundary condition is set by $u = -u_I$ on ∂D. The scatterer consists

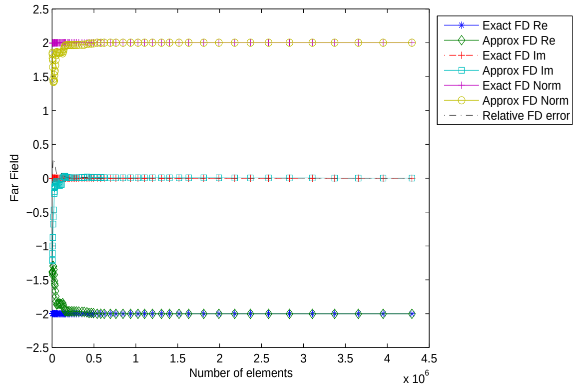

(a) Far-field pattern in direction (0,1,0).

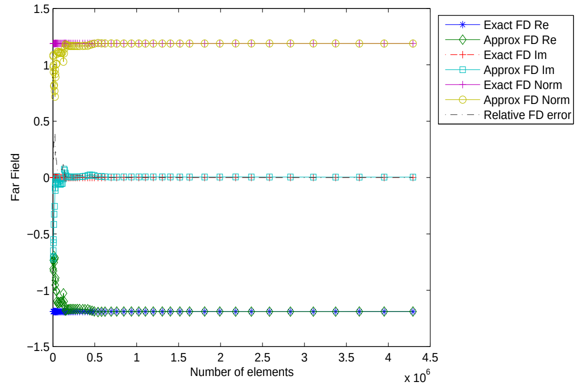

(b) Far-field pattern in direction (1,1,1).

Figure 5: Real part (FD Re), imaginary part (FD Im), and the norm (FD Norm) of the far-field pattern for Example 6.1.

of two L-shaped sub-scatterers D_1, D_2 and one U-shaped sub-scatterer D_3. The truncated domains are defined by $L_{1,m} = L_{2,m} = L_{3,m} = d_m = 0.5$ for $m = 1, 2, 3$.

Figure 6 shows $\log \eta_h$–$\log N_h$ curves for Example 6.2. The curve with "squares" shows the reduction rate of η_h obtained by the AAPML algorithm and the curve with "circles" shows the results by the adaptive PML method with global truncations. It indicates that both the AAPML algorithm and the adaptive PML method with global truncations yield quasi-optimal reduction rate of the a posteriori error estimates: $\eta_h \sim CN_h^{-2/3}$. Compared with Figure 2, Figure 6 indicates that the AAPML algorithm produces much less elements than the adaptive PML method with global truncations in the case of many sub-scatterers.

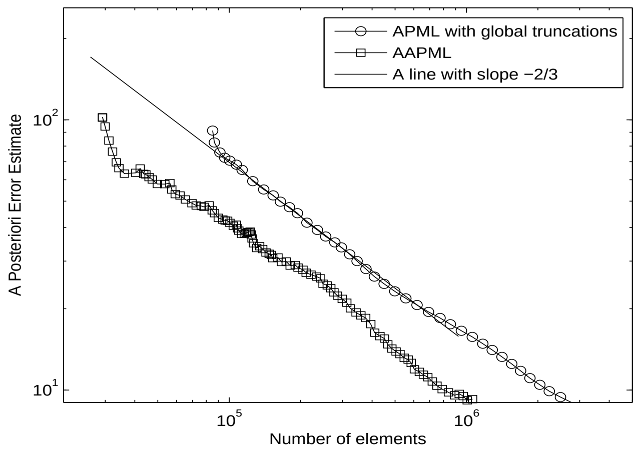

Figure 6: Quasi-optimality of adaptive PML methods for Example 6.2.

Figure 7 shows the real part of the numerical solution. It is clear that the solution decays very fast in the PML and becomes flat away from the inner boundary of the layer. Figure 8 shows the adaptively refined mesh with $143,486$ elements generated by the AAPML algorithm. Figure 9 shows the mesh on a slice of the domain which parallels to the x–z plane. Similar to Example 2, the mesh becomes much coarse away from the inner boundary of the PML due to the exponential decay of the solution.

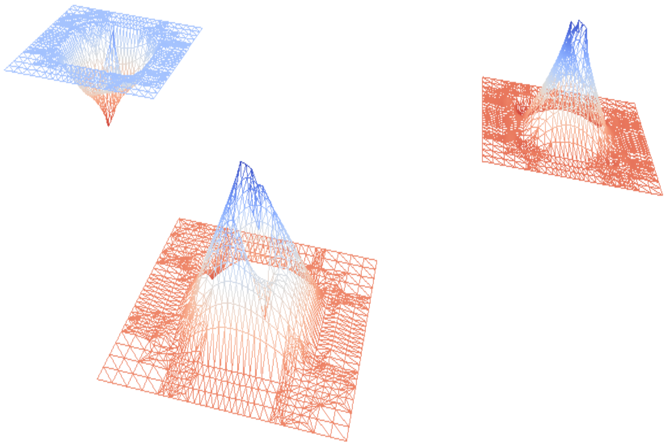

Figure 7: The real part of the solution of Example 6.2.

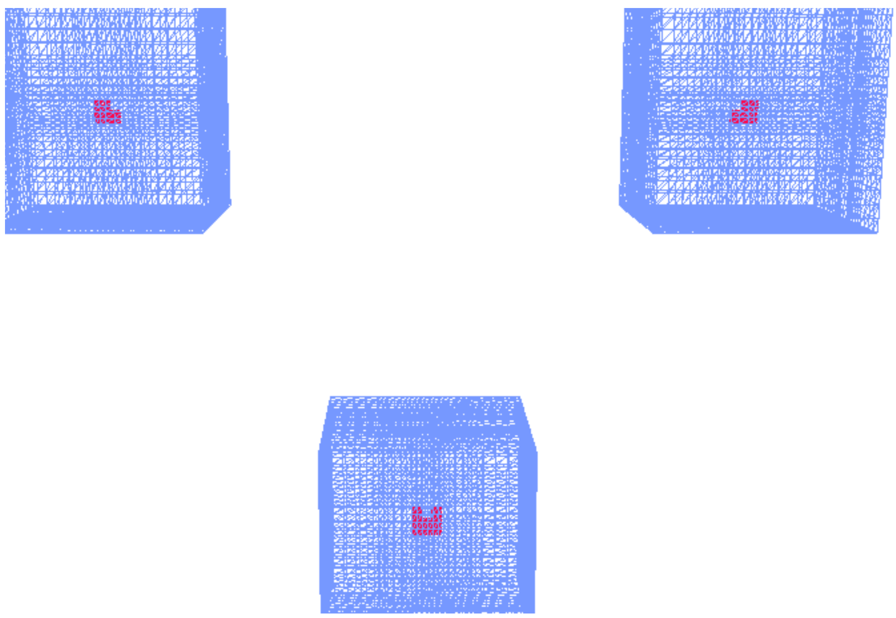

Figure 8: An adaptive mesh with $143,486$ elements produced by the AAPML algorithm for Example 6.2.

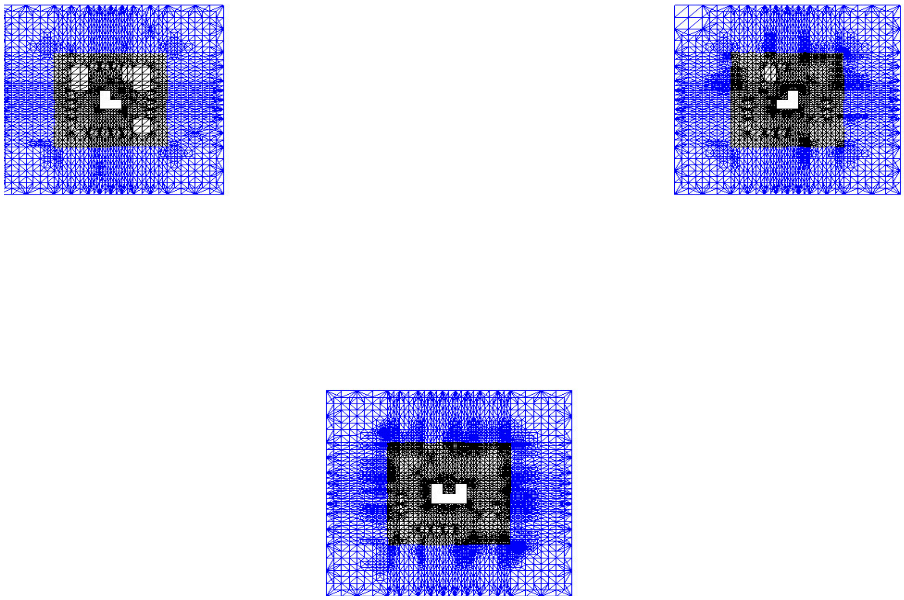

Figure 9: The slice of the mesh in Figure 8 cut by the x–z plane.

Example 6.3. As in Example 6.1, we consider the double scattering problem with two cubic sub-scatterers D_1, D_2 whose edge length is 0.2. The exact solution is chosen as

$$u(\boldsymbol{x}) = \frac{e^{\mathbf{i}kr_1}}{r_1} + \frac{e^{\mathbf{i}kr_2}}{r_2}, \qquad r_1 = |\boldsymbol{x} - \boldsymbol{c}_1|, \quad r_2 = |\boldsymbol{x} - \boldsymbol{c}_2|,$$

where $\boldsymbol{c}_1$, $\boldsymbol{c}_2$ are respectively the centers of the two sub-scatterers.

This example investigates how the convergence of the alternative iteration method depends on the distance between scatterers

$$\mathrm{d} = |\boldsymbol{c}_1 - \boldsymbol{c}_2| - 0.2\ .$$

To define the truncated domains B_1, B_2 and the computational domains O_1, O_2 in (19) and (26), we set $L_{1,m} = L_{2,m} = 0.2$ and $d_m = 0.1$ for $1 \le m \le 3$. Let (u_1^h, u_2^h) be the solution to the coupled discrete system (32). Let $\left(u_1^{n,h}, u_2^{n,h}\right)$ be the approximate solution of the block Gauss-Seidel scheme (36) or the alternative iteration scheme (37). We define the relative error by

$$e_n = \left(\left\|u_1^h - u_1^{n,h}\right\|^2_{H^1(\Omega_1)} + \left\|u_2^h - u_2^{n,h}\right\|^2_{H^1(\Omega_2)}\right)^{1/2} \left(\left\|u_1^h\right\|^2_{H^1(\Omega_1)} + \left\|u_2^h\right\|^2_{H^1(\Omega_2)}\right)^{-1/2}, \qquad n \ge 1.$$

In all computations of this example, the mesh $\mathcal{M}_1 \cup \mathcal{M}_2$ has 16416 elements and 48724 DOFs (see Fig. 10–12). Table 1 shows the convergence of the block Gauss-Seidel method (36) where the distance between two scatterers varies from d = 0.5 to d = 2.0. It holds asymptotically that

$$e_n \sim \mathrm{d}^{-2n}.$$

Heuristically this can also be seen from Lemma 4.1. In fact, from (37), computing $u_1^{n,h}$ from $u_1^{n-1,h}$ will use the wave propagation operators twice, i.e. $P_1\left(u_1^{n-1,h}\right)$ in computing $u_2^{n-1,h}$ and $P_2\left(u_2^{n-1,h}\right)$ in computing $u_1^{n,h}$. Then Lemma 4.1 indicates that the iterative error is reduced by a factor d^{-2}.

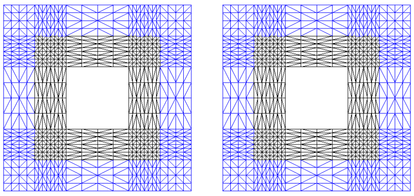

Figure 10: The mesh on slice $x_1 = 0$ of the domain. d = 0.5 .

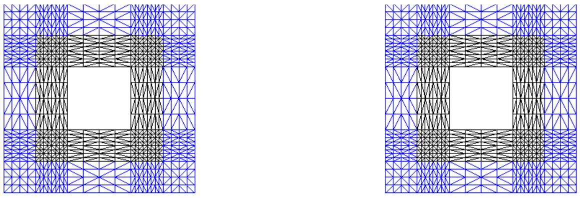

Figure 11: The mesh on slice $x_1 = 0$ of the domain. d = 1.0 .

Figure 12: The mesh on slice $x_1 = 0$ of the domain. d = 2.0 .

Remark 6.4. The PMLs in Example 6.1–6.2 are much thicker than the interior. They are resulted from the criterion for the PML reduction factor in Algorithm 6.1–6.2 :

$$\omega = \alpha_0^3(1+kL)^3 e^{-\gamma k\bar{\sigma}} < 10^{-8}.$$

This choice makes the truncation error of boundary conditions much smaller than numerical errors. We would like to give some comments on this point:

1. Choosing a thick PML, we show that the number of DOFs is insensitive to the thickness of PML for adaptive finite element method. From Figure 4 and 9 we find that the method yields very coarse meshes away from the inner boundary of the PML. Using adaptive finite element method, thick PML only yields a small number of additional DOFs compared with thin PML.

n	d = 0.5 e_n	e_n/e_{n-1}	d = 1.0 e_n	e_n/e_{n-1}	d = 2.0 e_n	e_n/e_{n-1}
1	1.42×10^{-1}		7.40×10^{-2}		4.19×10^{-2}	
2	3.31×10^{-3}	2.33×10^{-2}	5.26×10^{-4}	7.11×10^{-3}	7.50×10^{-5}	1.79×10^{-3}
3	8.38×10^{-5}	2.53×10^{-2}	3.63×10^{-6}	6.9×10^{-3}	1.35×10^{-7}	1.8×10^{-3}
4	2.12×10^{-6}	2.53×10^{-2}	2.66×10^{-8}	7.33×10^{-3}	5.57×10^{-9}	4.13×10^{-2}
5	5.45×10^{-8}	2.57×10^{-2}				

Table 1: Convergence of the block Gauss-Seidel method with respect to varying distance between two scatterers.

2. Setting $\omega < 10^{-8}$ is unnecessary for engineering computations. One wavelength is usually an acceptable thickness of PML in most cases.
3. The scatterers in our numerical experiments are unnecessarily very far from each other, especially for Example 6.3. They indicate that the method also works for relatively close scatterers.
4. For close scatterers, it holds on each adaptive mesh that

$$N_h \approx \sum_{i=1}^{I} N_i,$$

where N_h is the number of DOFs for global truncation which compasses all scatterers, and N_i is the number of DOFs of the mesh $\mathcal{M}_i$ for individual truncations (see Section 4.2). However, Algorithm 6.2 (AAPML) only amounts to one step of block Gauss-Seidel method for the algebraic system of the global truncation, whose block sizes are approximately $N_1, \cdots, N_I$.

Acknowledgement. The authors are grateful to Prof. Linbo Zhang and Dr. Tao Cui of the Institute of Computational Mathematics, Chinese Academy of Sciences for their help in the implementation of our algorithm. They also thank the anonymous referees for their constructive suggestions for the block Gauss-Seidel method in Section 5 and the last numerical experiment.

References

[1] B. Engquist and A. Majda, *Absorbing boundary conditions for the numerical simulation of waves*, Math. Comp., 31 (1977), pp 629–651.

[2] T. Hagstrom, *Radiation boundary conditions for the numerical simulation of waves*, Acta Numerica (1999), 47-106.

[3] D. Yu, *The Natural Boundary Integral Method and Its Applications*, Science Press & Kluwer Academic Publishers, 2002.

[4] M.J. Grote and C. Kirsch, *Dirichlet-to-Neumann boundary conditions for multiple scattering problems*, Journal of Computational Physics, 201(2004), pp. 630-650.

[5] J. P. Bérénger, *A perfectly matched layer for the absorption of electromagnetic waves*, J. Comput. Physics, 114 (1994), pp. 185-200.

[6] E. Turkel and A. Yefet, *Absorbing PML boundary layers for wave-like equations*, Appl. Numer. Math., 27 (1998), pp. 533-557.

[7] F.L. Teixeira and W.C. Chew, *Advances in the theory of perfectly matched layers*, in: W.C. Chew et al, (eds.), Fast and Efficient Algorithms in Computational Electromagnetics, pp. 283- 346, Artech House, Boston, 2001.

[8] T. Hohage, F. Schmidt, and L. Zschiedrich, *Solving time-harmonic scattering problems based on the pole condition. II: Convergence of the PML method*, SIAM J. Math. Anal., 35 (2003), pp. 547-560.

[9] M. Lassas and E. Somersalo, *Analysis of the PML equations in general convex geometry*, Proceeding of the Royal Society of Edinburg (2001), pp. 1183 - 1207.

[10] Z. Chen and X. Liu, *An adaptive perfectly matched layer technique for time-harmonic scattering problems*, SIAM J. Numer. Anal., 43(2005), pp. 645-671.

[11] Z. Chen and H. Wu, *An adaptive finite element method with perfectly matched absorbing layers for the wave scattering by periodic structures*, SIAM J. Numer. Anal., 41(2003), pp. 799-826.

[12] Z. Chen and X. Wu, *An adaptive uniaxial perfectly matched layer technique for Time-Harmonic Scattering Problems*, Numerical Mathematics: Theory, Methods and Applications, 1(2008), pp. 113-137.

[13] M.N. Guddati and K.-W. Lim, *Continued fraction absorbing boundary conditions for convex polygonal domains*, Int. J. Numer. Meht. Engng., 66 (2006), pp. 949-977.

[14] C. Michler, L. Demkowicz, J. Kurtz, and D. Pardo, *Improving the performance of perfectly matched layers by means of hp-ddaptivity*, Numerical Methods for Partial Differential Equations, 23 (2007), pp. 832-858.

[15] D. Pardo, L. Demkowicz, C. Torres-Verdín, and C. Michler, *PML enhanced with a self-adaptive goal-oriented hp-finite element method: simulation of through-casing borehole resistivity measurements*, SIAM J. Sci. Comput., 30 (2008), pp. 2948-2964.

[16] D. Colton and R. Kress, *Integral Equation Methods in Scattering Theory*, John Wiley & Sons, New York, 1983.

[17] D. Colton and R. Kress, *Inverse Acoustic and Electromagnetic Scattering Theory*, Second Edition, Springer, Berlin, New York, 1998.

[18] P. Monk, *Finite Elements Methods for Maxwell Equations*, Oxford University Press, 2003.

[19] Z. Chen and W. Zheng, *Convergence of the uniaxial perfectly matched layer method for time-harmonic scattering problems in two-layered media*, SIAM J. Numer. Anal., 48 (2010), pp. 2158-2185.

[20] G.F. Roach and B. Zhang, *The limiting-amplitude principle for the wave propagation problem with two unbounded media,* Math. Proc. Camb. Phil. Soc., 112 (1992), pp. 207-223.

[21] G. Bao and H. Wu, *Convergence analysis of the PML problems for time-harmonic Maxwell's equations*, SIAM J. Numer. Anal., 43 (2005), pp. 2121-2143.

[22] Ph. Clément, *Approximation by finite element functions using local regularization*, RAIRO Anal. Numer. 9 (1975), pp. 75-84.

[23] L.R. Scott and Z. Zhang, *Finite element interpolation of nonsmooth functions satisfying boundary conditions*, Math. Comp., 54 (1994), pp. 483C493.

[24] I. Babuška and A. Aziz, *Survey Lectures on Mathematical Foundations of the Finite Element Method*, in The Mathematical Foundations of the Finite Element Method with Application to the Partial Differential Equations, ed. by A. Aziz, Academic Press, New York, 1973, pp. 5-359.

[25] A.H. Schatz, *An observation concerning Ritz-Galerkin methods with indefinite bilinear forms*, Math. Comp. 28 (1974), pp. 959-962.

[26] L. Zhang, *A Parallel Algorithm for Adaptive Local Refinement of Tetrahedral Meshes Using Bisection*, State Key Laboratory of Scientific and Engineering Computing of Chinese Academy of Sciences, 2007. <http://lsec.cc.ac.cn/phg/>.

[27] L. Zhang, *A Parallel Algorithm for Adaptive Local Refinement of Tetrahedral Meshes Using Bisection*, Numer. Math.: Theor. Method Appl., 2 (2009), pp. 65C89.

[28] W. Döfler, *A convergent adaptive algorithm for Possion's equations*, SIAM J. Numer. Anal., 33 (1996), pp. 1106-1124.